BMC Cancer

RESEARCH

Open Access

APOL4-mediated intracellular cholesterol trafficking is essential for glioblastoma cell growth

Mingxiang Zhang[1], Tao Yang[2*] and Youcun Qian[1,2*]

Abstract

Background Dysregulated fatty acid metabolism is a key contributor to poor prognosis in glioma, and targeting cholesterol metabolism represents a promising therapeutic strategy. Apolipoprotein L4 (APOL4), a member of the Apolipoprotein L family, has been implicated in lipid metabolism, but its role in glioma remains unclear.

Methods RNA-sequencing were performed to analysis gene expression under exogenous cholesterol treatment. Comprehensive bioinformatics analyses were performed using CGGA datasets to evaluate APOL4 expression, clinical correlations, and prognostic significance in GBM. In vitro experiments, including CRISPR-Cas9 mediated APOL4 knockdown, MTT assays, wound healing assays and immunofluorescence were performed to validate the oncogenic role of APOL4. Xenograft mouse models were employed to validate tumor growth in vivo.

Results RNA-sequencing showed that exogenous cholesterol upregulated the expression of APOL4 in U-87 cells. Clinical database analysis revealed that APOL4 was significantly upregulated in human glioblastoma. Genetic depletion of APOL4 markedly suppressed glioblastoma cell proliferation in vitro and impaired xenograft tumor growth in vivo. Furthermore, APOL4 localized to late endosomes and lysosomes, where it likely facilitated the cytoplasmic transport of exogenous cholesterol, supporting tumor cell growth.

Conclusions Our study identifies APOL4 as a novel regulator of cholesterol trafficking in glioma cells, promoting glioblastoma progression. These findings highlight APOL4 as a potential therapeutic target for glioma treatment.

Keywords Glioblastoma, Cholesterol, APOL4, lipid transport

Introduction

Glioma is a malignant tumor that occurs in the brain or spinal cord and originates from glial cells in the brain, including astrocytes, oligodendrocytes and ependymal cells [1]. According to the classification of the World Health Organization (WHO), gliomas can be divided into four grades, of which grade I is benign and grade IV is the most malignant glioblastoma (GBM) [2]. The pathogenesis of glioma is not fully understood and may be related to the interaction of genetic susceptibility factors and external environmental factors, such as exposure to high doses of ionizing radiation and genetic mutations associated

*Correspondence:
Tao Yang
yangtao@sinh.ac.cn
Youcun Qian
ycqian@sinh.ac.cn
[1]School of Life Science and Technology, ShanghaiTech University, Shanghai 200031, China
[2]Shanghai Institute of Nutrition and Health, University of Chinese Academy of Sciences, Chinese Academy of Sciences, Shanghai 200031, China

with rare syndromes [3]. Treatment of gliomas usually involves surgical removal, radiation therapy, and chemotherapy [4]. Surgery is designed to remove as much of the tumor as possible without damaging important functional areas of the brain. Postoperative radiation therapy and chemotherapy may be required to reduce tumor size and control the disease. Despite various therapeutic approaches, the treatment of gliomas still remains a challenge, especially for high-grade gliomas such as glioblastoma, which have poor responses to treatments and poor prognosis [5]. To significantly improve overall survival in glioma patients, it is vital to comprehensively understand the biology of malignant gliomas and identify the crucial molecules involved in controlling tumor growth in order to design more effective treatment options.

Recently, growing evidence shows that metabolism reprogramming may play an important role in malignant tumor growth, which has opened new windows for cancer treatment [6, 7]. In the context of gliomas, lipid metabolism plays an important role in the occurrence and development, immune evasion, and treatment resistance of tumor [8]. Therefore, intervention in lipid metabolism pathways may provide new strategies for the treatment of gliomas [9]. Notably, as a vital component of cell membranes or a precursor to many hormones that are required for cell signaling and survival, cholesterol plays a crucial role in glioma malignancy [10]. Glioma cells require large amounts of cholesterol to support their rapid growth, and these cholesterol mainly rely on exogenous supply rather than self-synthesis [11]. In glioma therapy, cholesterol metabolism has emerged as a promising potential target. A large body of studies have revealed that different cholesterol metabolism targeting techniques, such as activating the LXR receptor to inhibit or promote cholesterol uptake or efflux, disrupting cellular cholesterol transport, inhibiting the SREBF signaling pathway, or blocking cholesterol esterification may retard the tumor growth [12–14]. However, given those targets are too general and shared by other healthy cells, targeting those common cellular cholesterol metabolism regulators may induce significant adverse effects, limiting its utility in clinical trials. Therefore, it's urgent and essential to identify some highly specific regulators of cholesterol metabolism in the tumor cells as opposed to normal cells.

Apolipoprotein L4 (APOL4) is a member of the apolipoprotein L family, a group of proteins implicated in lipid metabolism and membrane trafficking [15–17]. Previous studies have demonstrated that APOL1 is correlated with plasma cholesterol and participates in cholesterol efflux pathway [18]. Additionally, APOL1 and APOL3 have been extensively studied for their involvement in membrane remodeling. Nevertheless, the function of APOL4 remains largely unknown. Considering its structural similarity to other APOL family members, APOL4 may possess similar functional properties in lipid metabolism.

Here, we found that exogenous cholesterol upregulated APOL4. Notably, APOL4 expression was also significantly elevated in human glioblastoma tissues compared to normal brain tissues. We further demonstrated that APOL4 localized to the late endosomes and lysosomes, and facilitated exogenous cholesterol trafficking into the cytoplasm. APOL4 deficiency in the glioblastoma cell line U-87 suppressed the cell proliferation in vitro and tumor development in vivo. Conversely, APOL4 overexpression promoted cell proliferation and tumor growth in U-251 cells. Together, we identity APOL4 as a novel cholesterol metabolism regulator in glioma cells and a potential therapeutic target for glioblastoma treatment.

Materials and methods

Reagents and chemicals

Palmitic acid (#P0500), Oleic acid (#O1008), Cholesterol (#C8667) and Mouse monoclonal anti-Flag (DYKDDDDK) antibody (#F1804) were purchased from Sigma-Aldrich. Stearic acid (#HY-B2219), Filipin complex (#HY-N6716), U18666A (#HY-107433) were purchased from MCE. Fatty acid free BSA (#A602448) were purchased from Sangon Biotech. CholEsteryl BODIPY™ FL C12 (#C3927MP) was purchased from Thermo Fisher. Lovastatin (#S1729) and Methylthiazolyldiphenyl-tetrazolium bromide (MTT, #ST316) were purchased from Beyotime. Rabbit polyclonal anti-SREBF2 antibody (#28212-1-AP) was purchased from Proteintech. Rabbit monoclonal anti-Flag (DYKDDDDK) antibody (#14793), Rabbit monoclonal anti-LAMP1 antibody (#9091), Rabbit monoclonal anti-α/β-Tubulin antibody (#2148) and Rabbit monoclonal anti-GAPDH antibody (#5174) were purchased from Cell Signaling Technology. Mouse Anti-LBPA (BMP) antibody (#Z-PLBPA) was purchased from Echelon Biosciences.

Mice

BALB/c nude mice were purchased from GemPharmatech Co., Ltd. (Nanjing, China). Mice were maintained under specific pathogen-free conditions and subjected to experiments at the ages of 6–8 weeks old. All mice were housed in SPF facility with 12 h light/12 h dark cycle at steady room temperature (22–24 °C) with free access to water and food. Both male and female mice were used in this study. All animal studies were performed in compliance with the guide for the care and use of laboratory animals and were approved by the institutional biomedical research ethics committee of the Shanghai Institute of Nutrition and Health, Chinese Academy of Sciences.

Cell culture

U-87 (#HTB-14), K562 (#CRL-3344) and HEK293T (#CRL-3216) were obtained from the American Type Culture Collection (ATCC). U-251 (#09063001) was obtained from the European Collection of Authenticated Cell Cultures (ECACC). U-87, HEK293T and U-251 were maintained in Dulbecco's modified eagle medium (DMEM) supplemented with 10% fetal bovine serum, and 1% penicillin/streptomycin. K562 was maintained in Roswell Park Memorial Institute (RPMI) 1640 supplemented with 10% fetal bovine serum and 1% penicillin/streptomycin.

Plasmids

APOL4 (Refseq: NM_001386885.1) complementary DNA was PCR amplified from K562 cells and cloned into pLVX-IRES-puro lentiviral vector modified with C-flag tag. pLV-RFP-GFP-LC3 was a gift from Dr. Yikun Yao (Shanghai Institute of Nutrition and Health, Chinese Academy of Sciences, Shanghai, China).

Fatty acid/BSA complex solution Preparation

A 100 mM fatty acid stock solution was prepared in 0.1 M NaOH by heating at 70 °C in a shaking water bath as a stock. In an adjacent water bath at 55 °C, 10% (w/v) fatty acid free (FAF) BSA solution was prepared in ddH_2O. A 10 mM fatty acid/BSA solution was prepared by adding 5 mL 100 mM fatty acid solution to 45 mL 10% FAF-BSA solution at 55 °C in a shaking water bath, then vortex mixed for 1 min followed by an additional 10 min incubation at 55 °C. The fatty acid/BSA complex solution was cooled to room temperature and filtered through a 0.45 μm filter.

Quantitative real-time PCR

RNAs were extracted from cells using RNAiso reagent (Takara) according to the manufacturer's instructions and then reverse transcripted into cDNA by One-Step PrimeScript RT-PCR Kit (Takara). The cDNAs were used for real-time PCR analysis with the indicated primer sets and SYBR Green PCR Master Mix (YEASEN). Step One Plus Real-Time PCR devices (QuantStudio™ 7 Flex, Applied Biosystems) were used to conduct the PCR. The PCR settings were 95 °C for 1 min, then 40 cycles of denaturation at 95 °C for 5 s, followed by annealing and extension at 60 °C for 30 s. The expression of target genes was normalized to expression of housekeeping gene *HPRT*. Primers are listed in supplementary Table e1.

Cell proliferation

Cells were seeded into 48-well plates (2×10^4 cells per well) for 12 h. Different fatty acids (50–400 μM Cholesterol, 50 μM Palmitic acid, 50 μM Oleic acid and 50 μM Stearic acid) were added to each well and cultured for 2 to 6 days. U-87 empty vector (EV) and APOL4 knock-out (KO) cells were seeded into 48-well plates (2×10^4 cells per well) and cultured 2 to 8 days; U-251 EV and APOL4 overexpression (OE) cells were seeded into 48-well plates (1×10^4 cells per well) and cultured 1 to 3 day. 10 μL MTT (dissolved in ddH_2O at a concentration of 10 mg/mL) were added to each well and keep culture for 2–4 h. After twice washed by PBS, 100 μL DMSO were added to each well and the amount for formazan product was evaluated at OD 570 nm.

Bulk RNA-seq

Cells were treated by control and 200 μM Cholesterol for 8 h and RNAs were extracted from cells using RNAiso reagent (Takara) according to the manufacturer's instructions. RNA quality was then determined using the 5300 Bioanalyzer (Agilent) and quantified using the ND-2000. Only high-quality RNA samples (RIN ≥ 6.5) were used for sequencing library construction. RNA purification, reverse transcription, library construction, and sequencing were performed at GENEWIZ, Inc., China (Suzhou, China) according to the manufacturer's instructions. 1 μg total RNA was used for following library preparation. The poly(A) mRNA isolation was performed using Oligo(dT) beads. The mRNA fragmentation was performed using divalent cations and high temperature. Priming was performed using Random Primers. First strand cDNA and the second-strand cDNA were synthesized. The purified double-stranded cDNA was then treated to repair both ends and add a dA-tailing in one reaction, followed by a T-A ligation to add adaptors to both ends. Size selection of Adaptor-ligated DNA was then performed using DNA Clean Beads. Each sample was then amplified by PCR using P5 and P7 primers and the PCR products were validated. Then libraries with different indexs were multiplexed and loaded on an Illumina Novaseq6000 instrument for sequencing using a 2 × 150 paired-end (PE) configuration according to manufacturer's instructions. Raw data were processed by Cutadapt (V1.9.1) with default parameters. Clean reads were then aligned separately to the reference genome via software Hisat2 (v2.2.1). Differential expression genes (DEG) of two samples were identified wiith the DESeq2 Bioconductor package, a model based on the negative binomial distribution. DEGs with $|\log2FC| \geqq 1$ and FDR ≤ 0.05 were considered as significantly differentially expressed genes.

CRISPR-Cas9 knockout cell lines generation

The sgRNA targeting APOL4 were designed on the ChopChop website (https://chopchop.cbu.uib.no/) and cloned into the lentiCRISPRv2-puro vector. The positive lentiCRISPRv2 plasmids were transfected into U-87 cells with Lipofectamine 3000. Cells with successful transfection were screened by adding puromycin (1 μg/

ml) for 3 days and single clones were seeded into 96-well plates. Single clones were verified by the PCR fragments sequencing and Quantitative Real-time PCR. The sgRNA sequences are listed in supplementary Table e1.

Wound healing assay

U-87 EV and APOL4 KO cells stably expressing GFP were seeded into 6-well plates (2×10^6 cells per well) for 12 h and treated with 25 μM Mitomycin C for 1 h. A linear scratch was made using a 200 μL tip. Each well was washed with PBS 2 times and then cultured with 10% FBS DMEM for 24 to 48 h. After twice washed by PBS, cells were fixed by 4% paraformaldehyde in PBS and imaged under microscope (ECHO, RVL-100-G).

In vivo tumor models

5×10^6 U-87 or 2×10^6 U-251 cells in 100 μL of PBS were subcutaneously inoculated into the nude mice in the right flank. Tumor size was measured every 3 days with a Vernier caliper, and tumor volume was calculated by the modified ellipsoid formula: 0.52× length × $(\text{width})^2$. Mice were euthanized by carbon dioxide and tumors were harvested.

Flow cytometry measurements

U-87 cells were seeded into 24-well plates (2×10^5 cells per well) for 12 h. 2 μM CholEsteryl BODIPY™ FL C12 were added to each wells and cells were keep cultured for 2, 6, 12 h. Lipid probe uptake was measured using CytoFLEX LX. Fluorescence was collected in B525 channel.

Total cholesterol measurements

Total cholesterol was measured with Total cholesterol assay kit (Nanjing Jiancheng Bioengineering Institute, A111-1-1) according to manufacturer's instruction. Cells were washed twice with PBS and lysed in PBS containing 1% (v/v) TritonX-100 for 30 min on ice. The measurement was carried out in 96-cell plates. 250 μL working buffer was added to each cell containing 2.5 μL samples, PBS or standard and incubate for 10 min at 37 °C, then measured on a microplate reader at OD 500 nm.

Filipin staining

Cells cultured on glass coverslips were washed twice with PBS, fixed for 15 min at room temperature with 4% paraformaldehyde in PBS followed by three washes with PBS, and incubation with 30 μg/ml filipin in PBS in the dark for 2 h. cells were then washed three times with PBS and incubated with PI for 10 min followed by three washes with PBS, and incubation with DAPI for 10 min. after an additional three washes in PBS, slides were then mounted and imaged under microscope (Zeiss, Axio Imager A2).

Western blot

Cells were harvested and homogenized in RIPA buffer (beyotime, P0013B) supplemented with protease inhibitor cocktail (APExBIO, K1007), 1 mM Phenylmethylsulfonyl fluoride (Aladdin, P105539), 1 mM Sodium Orthovanadate (Sigma, S6508), 10 mM Sodium fluoride (Sigma, S7920). Protein concentrations of lysates were determined using the BCA Protein Assay Kit (Beyotime, P0012). Samples were separated by SDS-PAGE and transferred onto PVDF membranes (Merck, IPVH00010). Membranes were blocked with 5% (w/v) fat-free milk in Tris-buffered saline containing 0.1% (v/v) Tween 20 (TBST) for 1 h. The following primary antibodies: mouse anti-flag (1:1000), rabbit anti-α/β-Tubulin (1:5000), rabbit anti-SREBF2 (1:1000) and rabbit anti-GAPDH (1:5000) were used and incubated overnight at 4 °C and subsequently washed for three times with TBST. The membranes were incubated with HRP-conjugated secondary antibodies (JACKSON) for 1 h at room temperature. After another washing for three times with wash buffer, signals were detected by using Enhanced chemiluminescence (ECL) reagent (Share-Bio).

Immunofluorescent microscopy

Cells cultured on glass coverslips were washed twice with PBS, fixed for 15 min at room temperature with 4% paraformaldehyde in PBS followed by three washes with PBS. After permeabilization with 0.25% Triton X-100 in PBS for 15 min followed by three washes in PBS, cells were blocked with 5% BSA in PBS for 1 h. Then the following primary antibodies: mouse anti-flag (1:1000), rabbit anti-LAMP1 (1:1000), rabbit anti-flag (1:1000), mouse anti-LBPA (1:200) in 2% BSA were used and incubated overnight at 4 °C. Cells were then washed three times with PBS and incubated for 1 h at room temperature with Alexa Fluor −488- or 568-conjugated secondary antibody followed by three washes with PBS, and incubation with DAPI for 10 min. after an additional three washes in PBS, slides were then mounted and imaged under a Zeiss confocal laser scanning microscope (Zeiss, LSM 710) equipped with a 63X oil immersion objective.

GFP-LC3-RFP assay

U-87 WT and APOL4 KO cells stably expressing GFP-LC3-RFP were cultured on glass coverslips in a complete medium and treated cholesterol for 8 h. Cells were then washed twice with PBS, fixed for 15 min at room temperature with 4% paraformaldehyde in PBS followed by three washes with PBS, and incubation with DAPI for 10 min. after an additional three washes in PBS, slides were then mounted and examined under a Zeiss confocal laser scanning microscope (Zeiss, LSM 710) equipped with a 63X oil immersion objective.

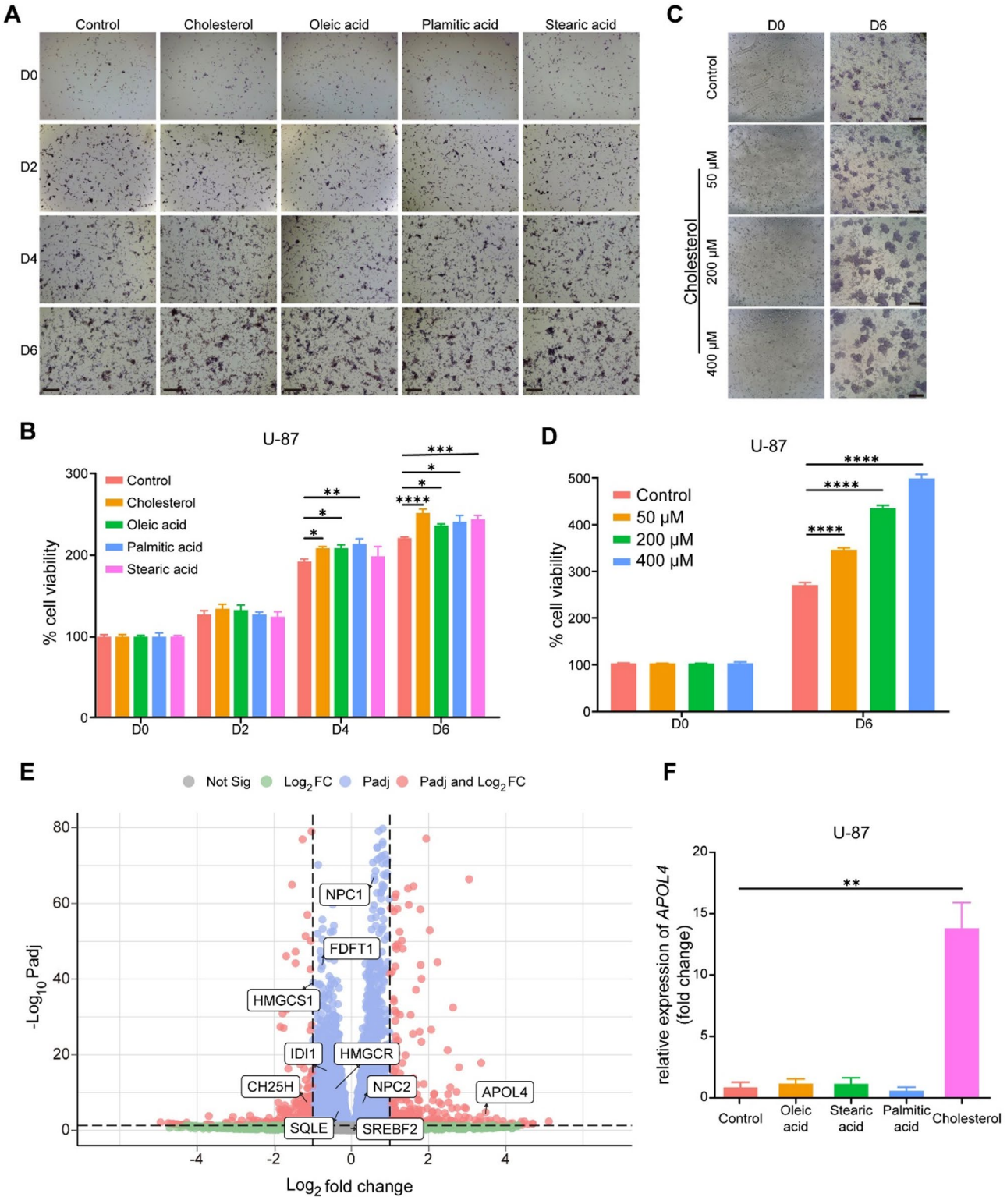

Fig. 1 (See legend on next page.)

(See figure on previous page.)

Fig. 1 Exogenous cholesterol induces APOL4 expression. **A**) Representative images of U-87 cells at day 0, 2, 4, 6 treated with control (DMEM with 10%FBS), adding extra Cholesterol (50 μM), Palmitic acid (50 μM), Oleic acid (50 μM) and Stearic acid (50 μM), then cultured with MTT for 4 h. Scale bars, 350 μm. **B**) The cell viability measured by MTT assay of U-87 cells at day 0, 2, 4, 6 treated with control (DMEM with 10%FBS), adding extra Cholesterol (50 μM), Palmitic acid (50 μM), Oleic acid (50 μM) and Stearic acid (50 μM). **C**) Representative images of U-87 cells at day 0 and day 6 treated with control (DMEM with 10%FBS), adding extra Cholesterol (50 μM, 200 μM, 400 μM), then cultured with MTT for 4 h. Scale bars, 350 μm. **D**) The cell viability measured by MTT assay of U-87 cells at day 0 and day 6 treated with control (DMEM with 10%FBS), adding extra Cholesterol (50 μM, 200 μM, 400 μM). **E**) Volcano plot of differentially expressed genes between control and cholesterol treatment (200 μM for 8 h) group of U-87 cells. **F**) Real-time quantitative PCR analysis of the expression of APOL4 mRNA in U-87 cells treated for 8 h with control (DMEM with 10%FBS), adding extra Cholesterol (200 μM), Palmitic acid (50 μM), Oleic acid (50 μM) and Stearic acid (50 μM). *$P < 0.05$, **$P < 0.01$, ***$P < 0.001$, ****$P < 0.0001$. Two-way ANOVA adjusted by Bonferroni's method (**B**, **D**), Two-tailed Student's t tests (**F**). Data are representative of three independent experiments (mean ± s.e.m.)

CGGA dataset analysis

Normalized RNA-seq and survival information of 693 glioma patients were employed from the Chinese Glioma Genome Atlas (CGGA, https://www.CGGA-argo.org).

Statistical analysis

Data are presented as the mean ± SEM. Differences between groups were evaluated by analysis of variance followed by a two-tailed unpaired Student's t-test with 95% confidence intervals, one-way analysis of variance (ANOVA) or by a two-way analysis of variance (ANOVA) with Bonferroni's multiple comparisons test. Survival curves were estimated using the Kaplan–Meier curves and compared with the log-rank test. p values < 0.05 were considered statistically significant. GraphPad Prism 10.0 software was used for statistical analysis.

Results

APOL4 was induced by exogenous cholesterol

In order to establish a system for in vitro screening of new regulators involved in cholesterol metabolism, we chose the well-established U-87 glioblastoma cell line as our model for investigation [19, 20]. We first supplied the U-87 cells with various lipids during cell culture, and then measured proliferation rate using the MTT assay. We confirmed that the proliferation of this type of glioma cell is heavily dependent on exogenous cholesterol in a dose-dependent manner (Fig. 1A-D), which is consistent with earlier findings [21, 22]. Then, we performed a transcriptome analysis of U-87 cells after the treatment with exogenous cholesterol. In addition to the down-regulation and up-regulation of certain well-known cholesterol synthesis and transport genes, we found APOL4, a novel lipoprotein with uncharacterized function, was strongly increased in this context (Fig. 1E). To further validate the transcriptome findings, we conducted real-time PCR analysis, which confirmed the marked increase in APOL4 expression following cholesterol supplementation, while other lipids had no effect (Fig. 1F).

APOL4 was upregulated in glioma

We then explored whether APOL4 expression is linked to the occurrence and progression of human glioma. Utilizing the CGGA database [23], we performed a comprehensive analysis of APOL4 mRNA levels across glioma and normal brain tissues. Our findings revealed that APOL4 expression is significantly elevated in GBM compared to both low-grade gliomas (LGG) and normal brain tissues (Fig. 2A). Furthermore, we observed a strong positive correlation between APOL4 expression and the WHO classification of glioma grades, with the highest expression found in WHO grade 4 gliomas (Fig. 2B). To further investigate the clinical relevance of APOL4, we compared primary and recurrent gliomas, which revealed that increased APOL4 expression is associated with poor prognosis (Fig. 2C). These results suggest that APOL4 may have a role in the aggressiveness and recurrence of gliomas. Additionally, we conducted a differential gene expression analysis between LGG and GBM tissue samples, illustrated by a volcano plot. APOL4, along with several previously identified poor prognosis-related genes, was found to be significantly upregulated in GBM compared to LGG (Fig. 2D). This indicates that APOL4 may be involved in a broader metabolic reprogramming in glioblastoma. Further analysis of the database revealed a correlation between APOL4 high expression and worse disease-free survival (DFS) in both primary and recurrent gliomas (Fig. 2E and F), indicating that higher levels of APOL4 may be linked to more aggressive disease and lower survival rates. In summary, these findings demonstrate that APOL4 is significantly upregulated in GBM that may contribute to its development and progression.

APOL4 deficiency inhibits U-87 cell growth in vitro

Given the elevated expression of APOL4 in GBM, we sought to determine its potential role in the occurrence and progression of human glioma. To investigate this, we employed CRISPR-Cas9 gene editing to specifically knock out the APOL4 gene in U-87 glioblastoma cells. We verified the deletion efficiency by genome PCR (Fig. 3A), as well as the significant reduction in APOL4 mRNA levels using real-time PCR (Fig. 3B). Since APOL4 was strongly induced by exogenous cholesterol as described above, we hypothesized that it may play a role in regulating cholesterol metabolism, which in turn could impact cell growth. To test this, we conducted a continuous assessment of the proliferation rates of wild-type

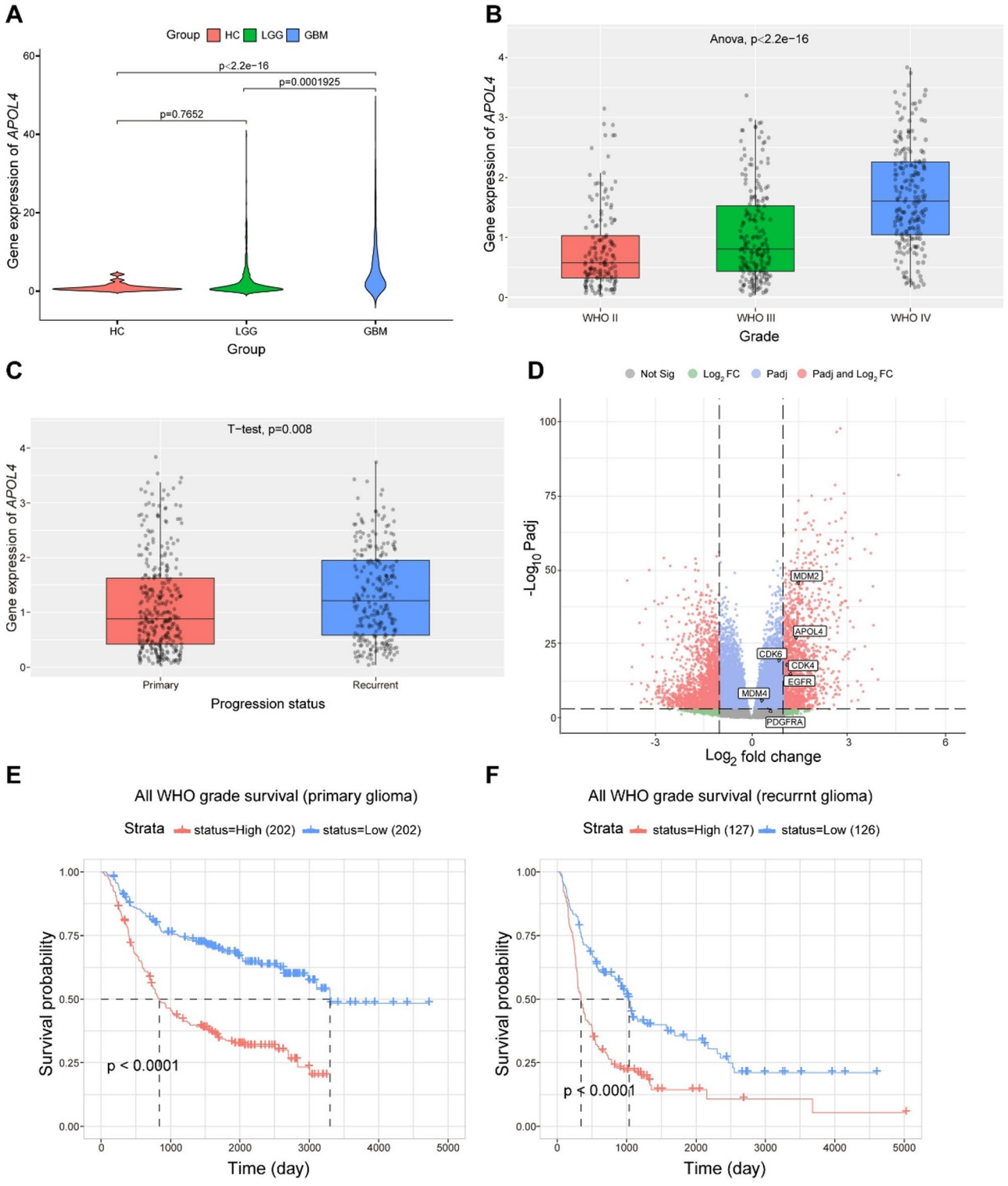

Fig. 2 A high level of APOL4 expression is associated with poor prognosis in glioma. **A**) The APOL4 expression in normal, LGG, GBM tissues in the CGGA database. **B**) The APOL4 expression in different WHO grades in gliomas in the CGGA database. **C**) The APOL4 expression in primary and recurrent gliomas in the CGGA database. **D**) Volcano plot of differentially expressed genes between LGG and GBM tissues in the CGGA database. **E**) The survival curve validating the correlation between the expression levels of APOL4 in primary glioma patients. **F**) The survival curve validating the correlation between the expression levels of APOL4 in recurrent glioma patients. Kruskal-Wallis test adjusted by Bonferroni's method (**A**), one-way ANOVA adjusted by Bonferroni's method (**B**), Two-tailed Student's t tests (**C**), or log-rank test (**E**, **F**)

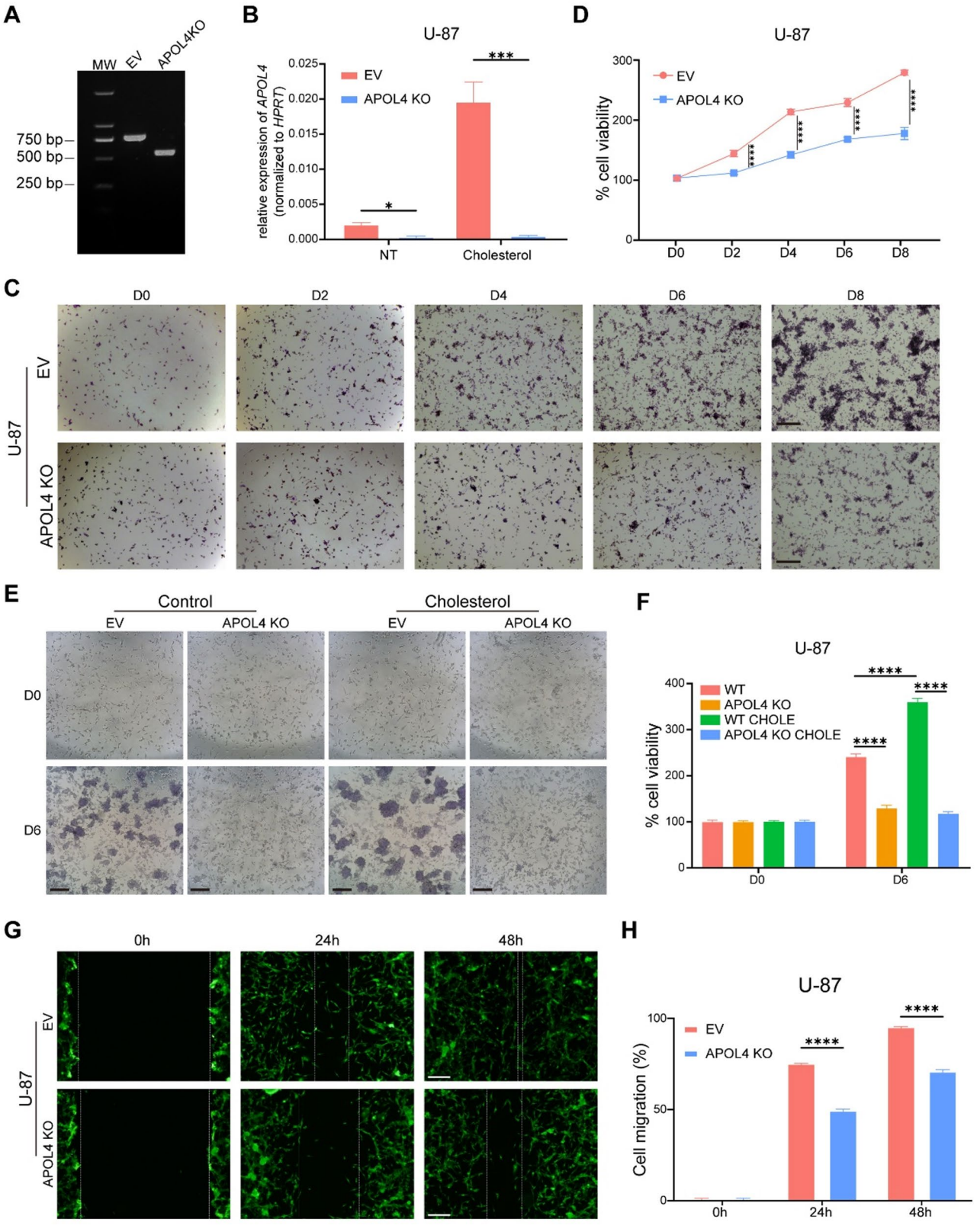

Fig. 3 (See legend on next page.)

(See figure on previous page.)

Fig. 3 APOL4 deficiency suppresses U-87 cell growth in vitro. **A**) The PCR confirmation of APOL4 knock out in U-87 cells; **B**) Real-time quantitative PCR analysis of the expression of APOL4 mRNA in EV and APOL4$^{-/-}$ U-87 cells treated with control and cholesterol (200 μM) for 8 h; **C**) Representative images of cell growth of EV and APOL4$^{-/-}$ U-87 cells at day 0, 2, 4, 6, 8. Scale bars, 350 μm. **D**) The cell viability measured by MTT assay of EV and APOL4$^{-/-}$ U-87 cells at day 0, 2, 4, 6, 8. **E**) Representative images of cell growth of EV and APOL4$^{-/-}$ U-87 cells treated with control (DMEM with 10%FBS) and cholesterol (200 μM) at day 0 and day 6. Scale bars, 350 μm. **F**) The cell viability measured by MTT assay of EV and APOL4$^{-/-}$ U-87 cells treated with control (DMEM with 10%FBS) and cholesterol (200 μM) at day 0 and day 6. **G**) Representative images of the wound healing assay of EV and APOL4$^{-/-}$ U-87 cells at 0, 24, 48 h. the white lines indicate the wound area. Scale bars, 200 μm. **H**) Quantification of the cell migration ratio of EV and APOL4$^{-/-}$ U-87 cells at 0, 24, 48 h. *$P < 0.05$, ***$P < 0.001$, ****$P < 0.0001$. Two-tailed Student's t tests (**B**) or two-way ANOVA adjusted by Bonferroni's method (**D**, **F**, **H**). Data are representative of three independent experiments (mean ± s.e.m.)

(WT) and APOL4-deficient U-87 cells under standard culture conditions. The results showed that APOL4 deficiency significantly impaired cell proliferation compared to the WT cells (Fig. 3C and D). Furthermore, the growth phenotype became significantly more pronounced under exogenous cholesterol treatment (Fig. 3E and F), reinforcing the hypothesis that APOL4 may function in a cholesterol-dependent manner. To further confirm the relationship between APOL4 function and exogenous cholesterol, we included a new cell line, U-251, which has almost no baseline expression of APOL4 (Figure S1A). We conducted the proliferation rates of WT and APOL4-overexpression U-251 cells under fatty acid-free culture conditions treated with exogenous cholesterol. The results showed that APOL4 overexpression significantly promoted cell proliferation (Figure S1C), verified that APOL4's functionality relies on the supplementation of exogenous cholesterol. To further explore the functional impact of APOL4 on glioma progression, we performed a wound healing assay to evaluate the collective cell migration and growth of APOL4-deficient versus WT U-87 cells. To enhance visualization under the microscope, we labeled the cells with constitutively expressed GFP. Our analysis revealed that APOL4-deficient U-87 cells exhibited a significantly slower migration rate compared to control cells (Fig. 3G and H). This reduced migratory capacity indicates that APOL4 not only supports cell proliferation but also influences the invasive and migratory behavior of GBM cells. In summary, these results demonstrate that APOL4 plays an important role in regulating cell proliferation and migration in glioblastoma.

APOL4 deficiency affects U-87 cell growth in vivo

After observing that APOL4-deficient U-87 cells exhibited poor growth in vitro, we next sought to determine whether this deficiency would similarly affect tumor development in vivo. To explore this, we employed a mouse xenograft tumor model and injected equal quantities of control and APOL4-deficient U-87 cells subcutaneously on the flank area of the nude mice. We monitored tumor growth over time by measuring the size and weight of the tumors. The results were striking—APOL4 deletion had a profound effect on tumor development, as evidenced by significantly slower tumor growth curves, smaller tumor size, and reduced tumor weight in the APOL4-deficient group compared to the control group (Fig. 4A-D). This dramatic reduction in tumorigenic capacity suggests that APOL4 is crucial for GBM cell proliferation and survival not only in vitro but also in the more complex environment of a living organism. Consistent with the results from U-87 models, tumor growth in vivo was significantly promoted in U-251 APOL4-OE cells (Fig. 4E-H). Taken together, these in vivo findings underscore the possibility that disrupting the tumor's dependence on APOL4 may be possible to inhibit tumor growth and progression.

APOL4 mediates intracellular cholesterol trafficking by localizing to the late endosomes or lysosomes

Given APOL4's significant involvement in boosting U-87 cell proliferation, we wondered whether it functions by affecting cholesterol metabolism. First, we investigated whether endogenous cholesterol metabolism is altered under APOL4 deficiency. Since Sterol Regulatory Element-Binding Transcription Factor 2 (SREBF2) is a key transcription factor regulating endogenous cholesterol metabolism, which could be cleaved to its nuclear form (n-SREBF2) in response to enhanced cellular demand for cholesterol, we began by assessing its protein levels. Our analysis revealed a slight increase in n-SREBF2 expression in APOL4-deficient cells (Fig. 5A), indicating a compensatory enhancement of cholesterol metabolism. Consistently, we observed upregulation of most cholesterol biosynthesis genes following the loss of APOL4 (Fig. 5B). As glioma cells primarily rely on exogenous supply rather than self-synthesis and APOL4 can be strongly induced by exogenous cholesterol, we speculated that APOL4, as a member of the Apolipoprotein L family, may have a high possibility to exert an action in exogenous cholesterol uptake, transport or esterification. To test this notion, we first investigated whether APOL4 deficiency may alter exogenous cholesterol absorption. Using BODIPY-tagged cholesterol probes for indication, we discovered that APOL4 deletion has no effect on exogenous cholesterol uptake (Fig. 5C and D). We then assessed the total cholesterol level of WT and APOL4-deficient cells and discovered that the baseline level remains the same (Fig. 5E), indicating that uptake or efflux of intracellular cholesterol is unaffected under normal cell culture conditions. Meanwhile, when endogenous cholesterol synthesis pathway

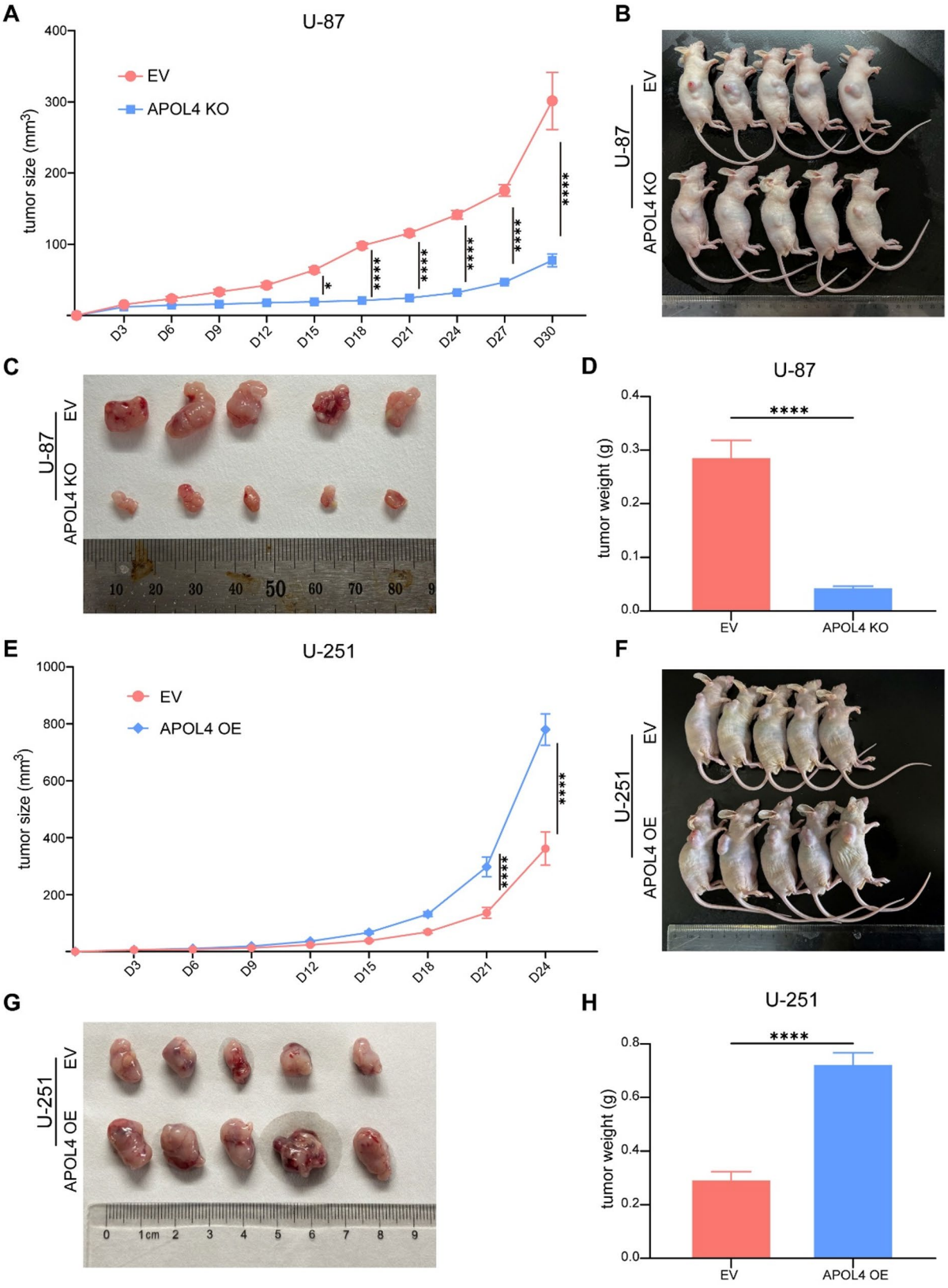

Fig. 4 (See legend on next page.)

(See figure on previous page.)

Fig. 4 APOL4 promotes GBM tumor growth in vivo. **A**) Average growth curves of EV and APOL4$^{-/-}$ U-87 tumors; $n=5$. **B**) Representative images of EV and APOL4$^{-/-}$ U-87 tumor-bearing BALB/c nude mice on day 30; $n=5$. **C**) Representative images of EV and APOL4$^{-/-}$ U-87 tumors on day 30; $n=5$. **D**) Tumor weight of EV and APOL4$^{-/-}$ U-87 tumor-bearing BALB/c nude mice on day 30; $n=5$. **E**) Average growth curves of EV and APOL4 overexpression (APOL4 OE) U-251 tumors; $n=5$. **F**) Representative images of EV and APOL4 OE U-251 tumor-bearing BALB/c nude mice on day 30; $n=5$. **G**) Representative images of EV and APOL4 OE U-251 tumors on day 24; $n=5$. **H**) Tumor weight of EV and APOL4 OE U-251 tumor-bearing BALB/c nude mice on day 24; $n=5$. $^{*}P<0.05$, $^{****}P<0.0001$. Two-tailed Student's t tests (D, H) or two-way ANOVA adjusted by Bonferroni's method (A, E). Data are representative of three independent experiments (mean ± s.e.m.)

was blocked by HMG CoA reductase inhibitor Lovastatin [24], the total cholesterol content of APOL4-deficient cells showed a slight increase as opposed to WT cells (Fig. 5E), suggesting that APOL4 is not a major contributor to endogenous production of cholesterol. However, the total intracellular cholesterol was greatly increased in APOL4-deficient cells when supplemented with more exogenous cholesterol (Fig. 5E). Interestingly, when we blocked the critical intracellular cholesterol trafficking regulator NPC1 either under basal culture conditions or during exogenous cholesterol supplementation, the intracellular cholesterol in both WT and APOL4$^{-/-}$ cells was increased to the same level (Fig. 5E). This inspired us to speculate that APOL4 may mediate intracellular cholesterol trafficking by acting on the downstream of NPC1 or in concert with NPC1. To verify the hypothesis, we observed that APOL4-deficient cells exhibited higher intracellular cholesterol accumulation compared to WT cells, as indicated by the non-esterified cholesterol-binding dye Filipin (Fig. 6A and B), displaying a phenotype strikingly similar to that of the well-known intracellular cholesterol transporter NPC1 [25–28]. Furthermore, immunofluorescence revealed that APOL4 was preferentially localized to late endosomes or lysosomes (Fig. 6C-E), with a distribution pattern very similar to NPC1 [29]. Previous studies have shown that loss of NPC1 induces cholesterol storage in lysosomes and impaired lysosome fusion with autophagosomes [30]. We wondered whether loss of APOL4 could lead to a similar phenotype. By exploiting a GFP-LC3-RFP reporter system [31], we found autophagosome formation after APOL4 depletion is greatly blocked under exogenous cholesterol stimuli (Fig. 6F). Taken together, those findings suggest that APOL4 may reside in the late endosomes or lysosomes to influence intracellular cholesterol transport.

Discussion

GBM is an aggressive brain or spinal cord cancer with poor prognosis and limited treatment options due to its heterogeneity, invasiveness, and the blood-brain barrier restricting drug delivery [32]. Conventional therapies have been inadequate, creating an urgent need for novel approaches [1]. Recent studies highlight the role of metabolic regulation in tumor growth and progression, offering potential therapeutic targets. In GBM, unique metabolic changes, especially in lipid metabolism, support rapid proliferation and treatment resistance [33]. GBM cells have an increased demand for lipids, particularly cholesterol, which is critical for cell membrane integrity and signaling [9]. Tumor cells enhance cholesterol uptake by upregulating LDL receptors or synthesizing it internally, while exporting excess cholesterol through transporters like ABCA1 and ABCG1 to avoid overload [34–36]. Targeting cholesterol metabolism—by inhibiting uptake and synthesis or promoting efflux—is being explored as a potential therapeutic strategy for GBM.

However, the studies on the cholesterol metabolism in GBM usually focus on the common regulators, which are shared and utilized by other healthy cells. Therefore, targeting those common regulators may potentially bring about severe adverse effects, restricting its use in therapeutic trials. Therefore, we wonder whether any new and specific cholesterol metabolism regulators could be identified. Given the intricate and complex niche in the carcinoma in situ, we chose to treat a routinely used GBM cell line U-87 with exogenous cholesterol in vitro. We first validated the growth-promoting role of cholesterol in U-87 cells compared to a variety of other lipids. Then, we performed a transcriptome analysis of U-87 cells after the treatment with exogenous cholesterol. Unexpectedly, when compared to previously known regulators (LDLR, NPC1, NPC2 etc.), we discovered that a lipoprotein, APOL4, is strongly up-regulated. Next, we evaluated the human glioblastoma transcriptome data from online database and identified that APOL4 is highly expressed in GBM tissues, with minimal expression in normal and LGG tissues, which is consistent with our RNA-seq results. Despite these promising findings, there are still several unanswered questions. First, it remains unclear which signaling pathway cholesterol activates to induce APOL4 expression. Cholesterol is known to engage multiple intracellular signaling networks, including the SREBF pathway, but whether APOL4 is regulated by SREBF2 or an alternative pathway remains to be elucidated. Understanding this mechanism is crucial for determining how cholesterol drives the upregulation of APOL4 in GBM cells and whether this can be targeted therapeutically. Second, while our experiments were conducted in cell lines and xenograft tumors, it is uncertain whether the same induction of APOL4 by exogenous cholesterol occurs in tumor cells of GBM patients. Given that brain cholesterol is primarily synthesized locally by astrocytes and is largely insulated from peripheral

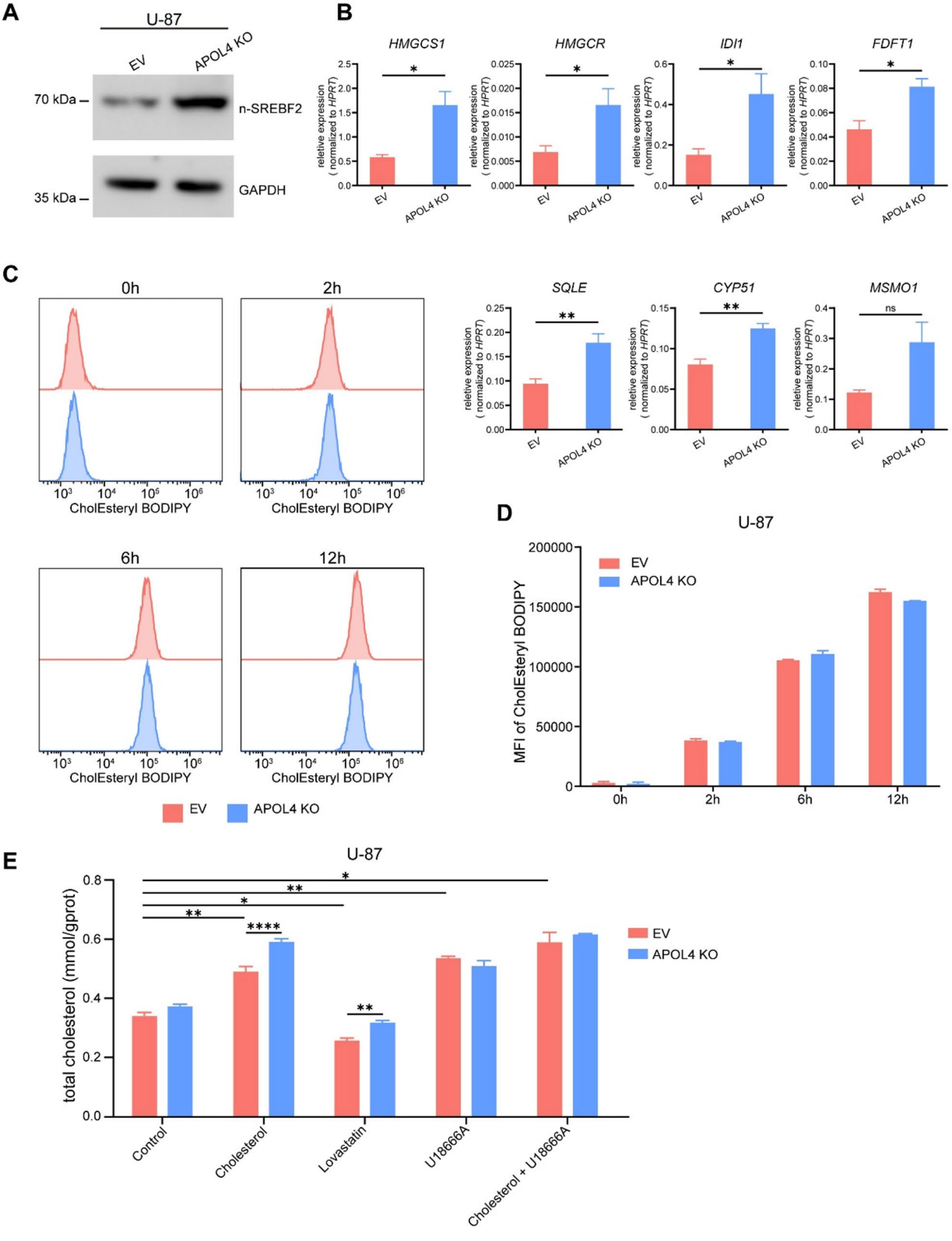

Fig. 5 (See legend on next page.)

(See figure on previous page.)

Fig. 5 APOL4 deficiency in U-87 cells upregulated endogenous cholesterol biosynthesis. **A**) Immunoblotting of n-SREBF2 in EV and APOL4$^{-/-}$ U-87 cells. **B**) Real-time quantitative PCR analysis of the expression of cholesterol biosynthesis genes in EV and APOL4$^{-/-}$ U-87 cells; **C**) Representative images of BODIPY-cholesterol probe uptake by flow cytometry in EV and APOL4$^{-/-}$ U-87 cells. **D**) Quantification of BODIPY-cholesterol probe uptake measurements by flow cytometry in EV and APOL4$^{-/-}$ U-87 cells. **E**) Intracellular concentration of total cholesterol in EV and APOL4$^{-/-}$ U-87 cells treated for 8 h with control, cholesterol (50 μM), lovastatin (5 μM), U18666A (2 μM), cholesterol (50 μM) + U18666A (2 μM). ns, not significant; *$P < 0.05$, **$P < 0.01$, ****$P < 0.0001$. Two-tailed Student's t tests (**B**) or two-way ANOVA adjusted by Bonferroni's method (**E**). Data are representative of three independent experiments (mean ± s.e.m.)

dietary cholesterol due to the brain blood barrier. it is critical to determine whether APOL4 expression is similarly elevated in GBM patients and modulated in patients undergoing systemic cholesterol-lowering therapies like statins. The absence of APOL4 homologs in mice further complicates this issue, as it restricts the ability to study this phenomenon in common preclinical mouse models of GBM. Consequently, tracing these changes in human subjects, possibly through patient-derived xenografts or advanced organoid models, will be essential for verifying the role of APOL4 in cholesterol metabolism in GBM.

So, what role does APOL4 perform in GBM cells? We believe it may have a favorable link with exogenous cholesterol. We wonder if APOL4 deficiency affects the proliferation of U-87 cells, which rely on cholesterol for fast growth. Consistent with our hypothesis, we discovered that APOL4 deletion in U-87 cells significantly reduces cell proliferation under normal culture conditions. Simultaneously, subcutaneous injection of APOL4-deficient U-87 cells into nude mice indicated that APOL4 deletion also inhibits tumor development. Similarly, APOL4 overexpression in U-251 cells promotes cell proliferation and tumor development. However, a technical limitation of our study is the use of subcutaneous rather than orthotopic xenografts, which do not fully replicate the brain's intrinsic environment, particularly the impact of intracranial cholesterol on tumor growth. Consequently, the observed tumor growth promoted by APOL4 may not fully recapitulate the clinical behavior of GBM. Future studies employing intracranial models would help validate our findings in a more physiologically relevant context. Then, we wonder how APOL4 function in the cholesterol metabolism. Given the identity of lipoprotein, we speculate that APOL4 may act on exogenous cholesterol uptake, transport or esterification. Notably, APOL4 belongs to the apolipoprotein L family which is known to participate in lipid binding and membrane remodeling, suggesting its potential role in intracellular cholesterol handling through direct lipid interaction. We initially investigated the efficiency of exogenous cholesterol uptake and discovered that APOL4 deficiency has no influence on it. Then, we examined the total intracellular cholesterol level under various settings and discovered that it rises when exposed to more exogenous cholesterol. This phenotype resembles defects seen in lysosomal cholesterol transport disorders, implicating APOL4 in post-uptake processes. Furthermore, intracellular non-esterified cholesterol staining has shown that there is more deposited cholesterol in APOL4-deficient cells, indicating impaired mobilization of internalized cholesterol rather than defective absorption. Given that APOL4 shares structural features with other APOLs, particularly pore-forming and lipid-binding domains, we hypothesized it might facilitate cholesterol extraction from lysosomes. To probe its mechanism, we determined APOL4's subcellular localization. We observed that APOL4 may target the late endosome and lysosome in a fashion very similar to the traditional intracellular cholesterol transporter NPC1. This colocalization, coupled with the cholesterol accumulation phenotype, suggests functional crosstalk between the two proteins. Subsequently, we confirmed that APOL4 deletion can impede autophagosome formation. Based on these observations, we speculate that APOL4 may cooperate with NPC1 to facilitate the trafficking of exogenous cholesterol from lysosomes to other organelles. However, there are several questions unanswered. First, it is unknown whether APOL4 could directly bind to cholesterol in the late endosome or lysosome. Second, it's unclear that whether APOL4 truly interacts with NPC1 despite the fact that they all reside in the same organelles. Finally, it remains challenging to figure out how APOL4 collaborates with NPC1 to fulfill the task of handling cholesterol transport. All of these questions require more investigation.

In addition, cholesterol metabolism is also related to immunotherapy of GBM [22]. Changes in cholesterol metabolism may affect the function of immune cells, thereby affecting the immune microenvironment of tumors [37]. For example, the combination of cholesterol metabolism inhibitors with tumor vaccine immunotherapy has shown clinical promise in some studies [38, 39]. Notably, glioma cells may affect immune cells in the tumor microenvironment, such as microglia, by regulating cholesterol metabolism [40]. These cells play an important role in the immune microenvironment of glioma, and their cholesterol metabolism characteristics and metabolic dysregulation may lead to the formation of an immunosuppressive microenvironment. Thus, it may be very interesting to further explore any alterations in immune microenvironment when the function of APOL4 is blocked in the GBM cells.

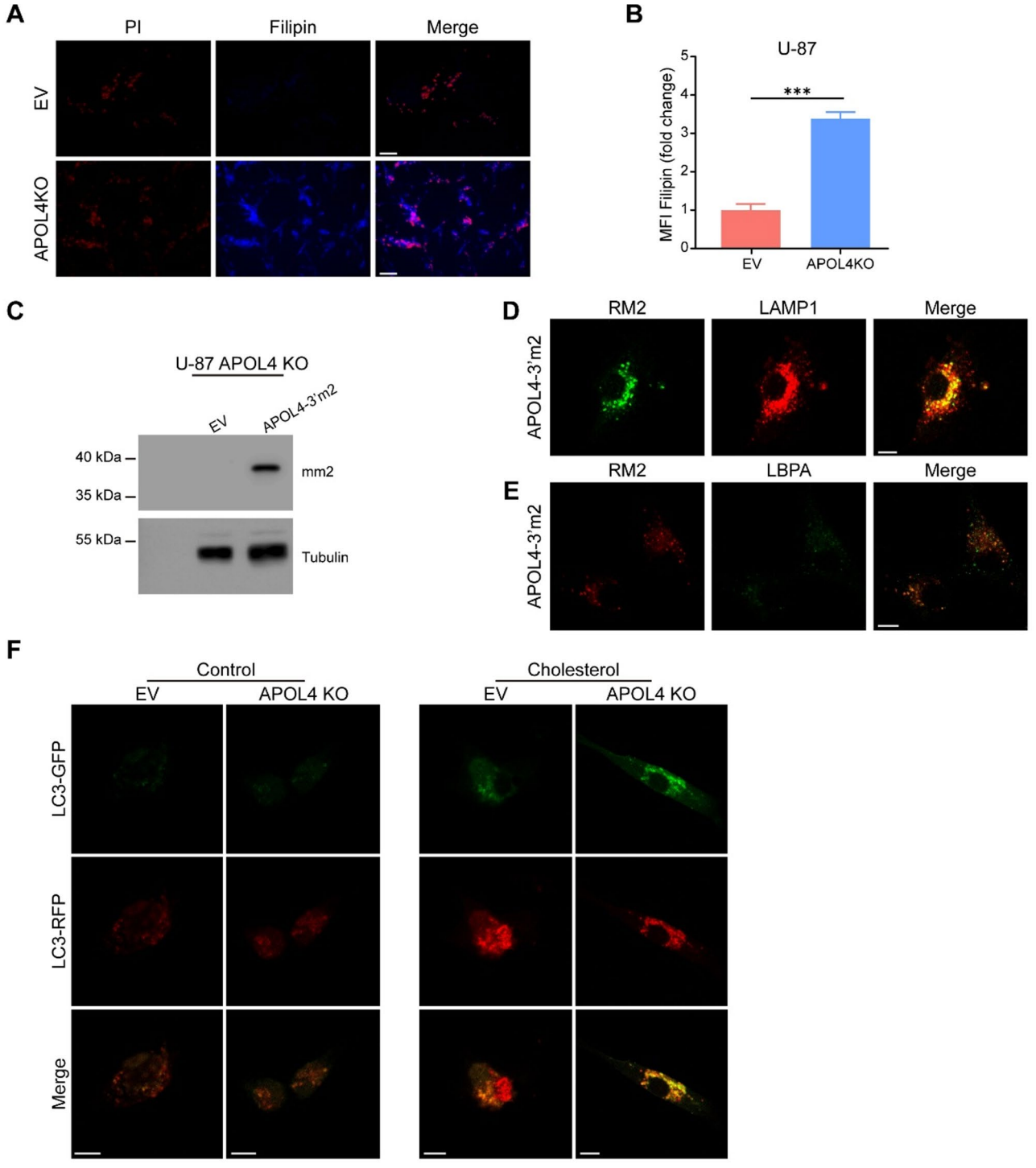

Fig. 6 APOL4 localize to late endosomes and lysosomes to facilitate the transport of exogenous cholesterol to the cytoplasm. **A**) Representative images of filipin staining validating free cholesterol of WT and APOL4$^{-/-}$ U-87 cells. Scale bars, 40 μm. **B**) Quantification of filipin staining (MFI) of EV and APOL4$^{-/-}$ U-87 cells. **C**) Immunoblotting of APOL4 in EV and APOL4 reconstituted APOL4$^{-/-}$ U-87 cells. **D**) Immunofluorescence of APOL4 and LAMP1 localization in APOL4-Flag stably reconstituted APOL4$^{-/-}$ U-87 cells. Scale bars, 10 μm. **E**) Immunofluorescence of APOL4 and LBPA localization in APOL4-Flag stably reconstituted APOL4$^{-/-}$ U-87 cells. Scale bars, 10 μm. **F**) Autophagy flux detected by RFP-GFP-LC3 system in EV and APOL4$^{-/-}$ U-87 cells treated for 8 h with control and cholesterol (50 μM). Scale bars, 10 μm. ***$P < 0.001$. Two-tailed Student's t tests. Data are representative of three independent experiments (mean ± s.e.m.)

Supplementary Information

The online version contains supplementary material available at https://doi.org/10.1186/s12885-025-14316-4.

Supplementary Material 1

Supplementary Material 2

Supplementary Material 3

Acknowledgements
This work was supported by grants from the National Key R&D Program of China (2020YFA0509100) and the National Natural Science Foundation of China (32030039). We thank Dr. Yikun Yao for plasmids sharing.

Author contributions
Y.Q. and T.Y. supervised the research; T.Y., M.Z., and Y.Q. wrote the manuscript; M.Z. conducted the experiments and analyzed the data.

Funding
This work was supported by grants from the National Key R&D Program of China (2020YFA0509100) and the National Natural Science Foundation of China (32030039).

Data availability
The bulk RNA-seq data are available in the NCBI database under BioProject ID: PRJNA1172562.

Declarations

Ethics approval and consent to participate
All animal studies were performed in compliance with the guide for the care and use of laboratory animals and were approved by the institutional biomedical research ethics committee of the Shanghai Institute of Nutrition and Health, Chinese Academy of Sciences.

Consent for publication
Not applicable.

Competing interests
The authors declare no competing interests.

Abbreviations.
Not applicable.

Received: 19 November 2024 / Accepted: 12 May 2025
Published online: 21 May 2025

References

1. Schaff LR, Mellinghoff IK. Glioblastoma and other primary brain malignancies in adults: A review. JAMA. 2023;329(7):574–87.
2. Bjorkblom B, et al. Distinct metabolic hallmarks of WHO classified adult glioma subtypes. Neuro Oncol. 2022;24(9):1454–68.
3. Goodenberger ML, Jenkins RB. Genetics of adult glioma. Cancer Genet. 2012;205(12):613–21.
4. Lee JH, Wee CW. Treatment of adult gliomas: A current update. Brain Neurorehabil. 2022;15(3):e24.
5. Rossmeisl JH. Novel Treatments for Brain Tumors. Vet Clin North Am Small Anim Pract. 2025;55(1):81–94.
6. Phan LM, Yeung SC, Lee MH. Cancer metabolic reprogramming: importance, main features, and potentials for precise targeted anti-cancer therapies. Cancer Biol Med. 2014;11(1):1–19.
7. Navarro C, et al. Metabolic reprogramming in Cancer cells: emerging molecular mechanisms and novel therapeutic approaches. Pharmaceutics. 2022;14(6).
8. Kou Y, Geng F, Guo D. Lipid metabolism in glioblastoma: from de Novo synthesis to storage. Biomedicines. 2022;10(8).
9. Cortes Ballen AI, et al. Metabolic reprogramming in glioblastoma multiforme: a review of pathways and therapeutic targets. Cells. 2024;13(18).
10. Huang B, Song BL, Xu C. Cholesterol metabolism in cancer: mechanisms and therapeutic opportunities. Nat Metab. 2020;2(2):132–41.
11. Miska J, Chandel NS. Targeting fatty acid metabolism in glioblastoma. J Clin Invest. 2023;133(1).
12. Geng F, et al. SREBP-1 upregulates lipophagy to maintain cholesterol homeostasis in brain tumor cells. Cell Rep. 2023;42(7):112790.
13. Sun Y, et al. Targeting cholesterol homeostasis through inhibiting SREBP-2: an Achilles' heel for glioblastoma. Neuro Oncol. 2023;25(11):2100–2.
14. Ramalingam PS, et al. Liver X receptors (LXRs) in cancer-an Eagle's view on molecular insights and therapeutic opportunities. Front Cell Dev Biol. 2024;12:1386102.
15. Duchateau PN, et al. Apolipoprotein L gene family: tissue-specific expression, splicing, promoter regions; discovery of a new gene. J Lipid Res. 2001;42(4):620–30.
16. Li Q, et al. Distribution and effect of apoL-I genotype on plasma lipid and Apolipoprotein levels in Chinese normalipidemic and endogenous hypertriglyceridemic subjects. Clin Chim Acta. 2009;403(1–2):152–5.
17. Wang Y, et al. ApoL6 associates with lipid droplets and disrupts Perilipin1-HSL interaction to inhibit lipolysis. Nat Commun. 2024;15(1):186.
18. Ryu JH, et al. APOL1 renal risk variants promote cholesterol accumulation in tissues and cultured macrophages from APOL1 Transgenic mice. PLoS ONE. 2019;14(4):e0211559.
19. Allen M, et al. Origin of the U87MG glioma cell line: good news and bad news. Sci Transl Med. 2016;8(354):354re3.
20. Ghiasvand S, et al. Transcriptome analysis evinces anti-neoplastic mechanisms of hypericin: A study on U87 glioblastoma cell line. Life Sci. 2021;266:118874.
21. Rios-Marco P, et al. Alkylphospholipids deregulate cholesterol metabolism and induce cell-cycle arrest and autophagy in U-87 MG glioblastoma cells. Biochim Biophys Acta. 2013;1831(8):1322–34.
22. Guo X, et al. Cholesterol metabolism and its implication in glioblastoma therapy. J Cancer. 2022;13(6):1745–57.
23. Zhao Z, et al. Chinese glioma genome atlas (CGGA): A comprehensive resource with functional genomic data from Chinese glioma patients. Genomics Proteom Bioinf. 2021;19(1):1–12.
24. Chan DY, et al. Lovastatin sensitized human glioblastoma cells to TRAIL-induced apoptosis. J Neurooncol. 2008;86(3):273–83.
25. Davidson CD, et al. Chronic cyclodextrin treatment of murine Niemann-Pick C disease ameliorates neuronal cholesterol and glycosphingolipid storage and disease progression. PLoS ONE. 2009;4(9):e6951.
26. Tamura A, Yui N. Lysosomal-specific cholesterol reduction by biocleavable Polyrotaxanes for ameliorating Niemann-Pick type C disease. Sci Rep. 2014;4:4356.
27. Brown A, et al. PEG-lipid micelles enable cholesterol efflux in Niemann-Pick type C1 disease-based lysosomal storage disorder. Sci Rep. 2016;6:31750.
28. Hoglinger D, et al. NPC1 regulates ER contacts with endocytic organelles to mediate cholesterol egress. Nat Commun. 2019;10(1):4276.
29. Colombo A, et al. Loss of NPC1 enhances phagocytic uptake and impairs lipid trafficking in microglia. Nat Commun. 2021;12(1):1158.
30. Elrick MJ, et al. Impaired proteolysis underlies autophagic dysfunction in Niemann-Pick type C disease. Hum Mol Genet. 2012;21(22):4876–87.
31. Kaizuka T, et al. An autophagic flux probe that releases an internal control. Mol Cell. 2016;64(4):835–49.
32. Torrisi F, et al. The hallmarks of glioblastoma: heterogeneity, intercellular crosstalk and molecular signature of invasiveness and progression. Biomedicines. 2022;10(4).
33. Zhao J, et al. Advancing glioblastoma treatment by targeting metabolism. Neoplasia. 2024;51:100985.
34. Maletinska L, et al. Human glioblastoma cell lines: levels of low-density lipoprotein receptor and low-density lipoprotein receptor-related protein. Cancer Res. 2000;60(8):2300–3.
35. Chen YH, et al. ABCG1 maintains high-grade glioma survival in vitro and in vivo. Oncotarget. 2016;7(17):23416–24.
36. Wang SM, et al. CCAAT/Enhancer-binding protein delta mediates glioma stem-like cell enrichment and ATP-binding cassette transporter ABCA1 activation for Temozolomide resistance in glioblastoma. Cell Death Discov. 2021;7(1):8.
37. Wang Y, et al. Lipid metabolism and tumor immunotherapy. Front Cell Dev Biol. 2023;11:1187989.
38. Bader JE, Voss K, Rathmell JC. Targeting metabolism to improve the tumor microenvironment for Cancer immunotherapy. Mol Cell. 2020;78(6):1019–33.

39. Zhang H, et al. Cholesterol metabolism as a potential therapeutic target and a prognostic biomarker for Cancer immunotherapy. Onco Targets Ther. 2021;14:3803–12.
40. Sharma P, et al. Tumor microenvironment in glioblastoma: current and emerging concepts. Neurooncol Adv. 2023;5(1):vdad009.

Publisher's note